JOURNAL OF APPLIED ELECTROCHEMISTRY 10 (1980) 799–806

The impedance of the Leclanché cell. III. The impedance of the cell at different stages of discharge and state-of-charge indication by the impedance method

S. A. G. R. KARUNATHILAKA, N. A. HAMPSON

Department of Chemistry, University of Technology, Loughborough, Leicestershire, UK

R. LEEK

Department of Electronic and Electrical Engineering, University of Technology, Loughborough, Leicestershire, UK

T. J. SINCLAIR

Procurement Executive, Ministry of Defence, Royal Armament Research and Development Establishment, Fort Halstead, Sevenoaks, Kent, UK

Received 8 February 1980

The prediction of the residual capacity of some primary electrochemical storage cells has been investigated using the impedance technique over an extensive frequency range. The frequency responses of Leclanché cells in various states of charge are presented and it is shown that the gross changes in impedance which result from discharging provide an adequate parameter for state-of-charge prediction. The component factors of the whole-cell impedance have been investigated and the contributions of the various cell components to the resultant frequency-response (resistive and reactive) spectrum identified. A knowledge of these contributions is important for the development of a suitable device for the rapid testing of cell quality since in principle the examination of each mode of failure of each component demands a separate test. In practice the understanding of the frequency response of the cell has enabled us to construct a relatively simple instrument which gives an adequate estimate of cell condition for ordnance applications. A block schematic diagram is presented and the operation of the device is described in principle.

1. Introduction

We have recently reviewed the published work on the impedance of storage cells [1] and shown how the impedance method may be expected to yield a powerful method for the estimation of state-of-charge in spite of the fact that most of the existing investigations involved secondary cells. In a subsequent publication [2] we have studied the impedance of fully charged Leclanché cells and shown that the frequency response over an extended range can be interpreted in terms of well-established electrochemical theory. Our interpretation has been confirmed by studying the electrochemistry of the separate electroactive components of the Leclanché cell [3].

The current growth in the use of electronics in military equipment has resulted in greater demands being made on the performance and reliability of the power sources required to operate portable kits. A wide range of hardware is powered by primary batteries, either with the battery sealed into the unit or with the facility to replace the battery when necessary. Present policy is to renew the battery or unit periodically or whenever there is doubt about the operational reliability of the battery. This system results in a high wastage rate of partially discharged but still usable batteries.

0021–891X/80/060799–08$02.80/0

A simple, rapid and reliable check on the energy available in a power source before committing the equipment to a mission would give the user greater confidence in the operational capability of the unit and reduce the level of battery procurement. Existing battery test equipments are not sufficiently accurate to predict the residual capacity in batteries with ease and confidence. A capacity meter allowing more precise measurement of the amount of usable energy in a cell would be a valuable asset for the exacting requirements of ordnance and military applications. The objective of this study was to identify a suitable, sensitive parameter in specific electrochemical systems and develop this into a practical device capable of predicting with precision the residual capacity in primary batteries of unknown storage and discharge history.

2. Experimental

Cell impedance determinations were made using a frequency response analyser (Solartron Type 1170) commanded by a potential controller (Kemitron PC-03). The impedance data were retrieved from the analyser as in-phase (Z') and out-of-phase (Z'') components and recorded on punched tape.

Cells (Ever Ready Type SP11) were discharged galvanostatically using an accurate galvanostat (Kemitron P-2-40-50) which incorporated a coulometer in order to record the charge automatically. Most discharges were carried out at the approximately nominal 100 h rate (25 mA). The states-of-charge of the cells were computed from the charge extracted and tested both immediately following the discharge and after a rest.

In order to obtain the impedance, the cell was poised at the reversible (terminal) potential using the potential controller. The frequency response analyser then automatically measured the impedance components at a series of frequencies in the range 10 kHz–0.1 mHz (ω the angular frequency $= 2\pi \times$ frequency). It should be noted that the perturbing a.c. had an amplitude of $\pm$ 2.5 mV; at very low frequency even this small signal changes the impedance: at our lower level of significance 1 mHz this change was small over the integration time used (100 cycles).

Acquired data were read into the computer (Prime 400) from the punched tape output and filed there. Sluyters [4] plots (Z' versus Z'') and Randles [5] plots (in-phase and out-of-phase component versus $\omega^{-1/2}$) were constructed for each impedance spectrum measured and subsequent calculations and graphical representations were drawn using the appropriate computer peripheral.

3. Results and discussion

Fig. 1 shows the Sluyters plot for an undischarged Leclanché cell. The form of the plot is identical to those which we have discussed in earlier papers [1] and represents a system controlled almost completely by the processes of charge transfer at a planar electrode and mass transport of the charge transfer products in a solution. The linear tail of the plot at low frequency, angled almost exactly $\pi/4$ to the real axis, confirms that the electrode is not initially porous. It is of interest that cells which have been in our store for some time develop some porosity of the zinc electrode caused by pitting corrosion; this is evinced from the reduction of the slope of the tail (a slope of $\pi/8$ is characteristic of a semi-infinite pore length). The diameter θ of the

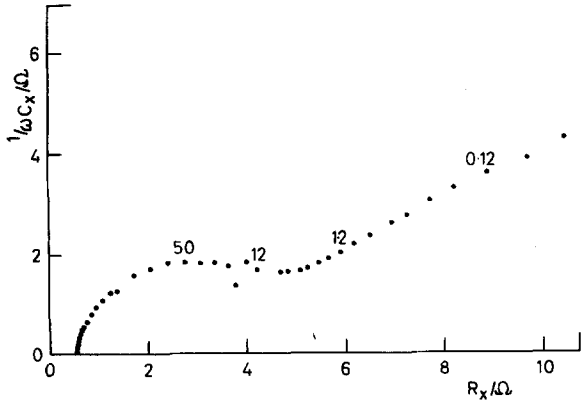

Fig. 1. Sluyters plot for new, undischarged SP11 cell. Numbers adjacent to points refer to frequency.

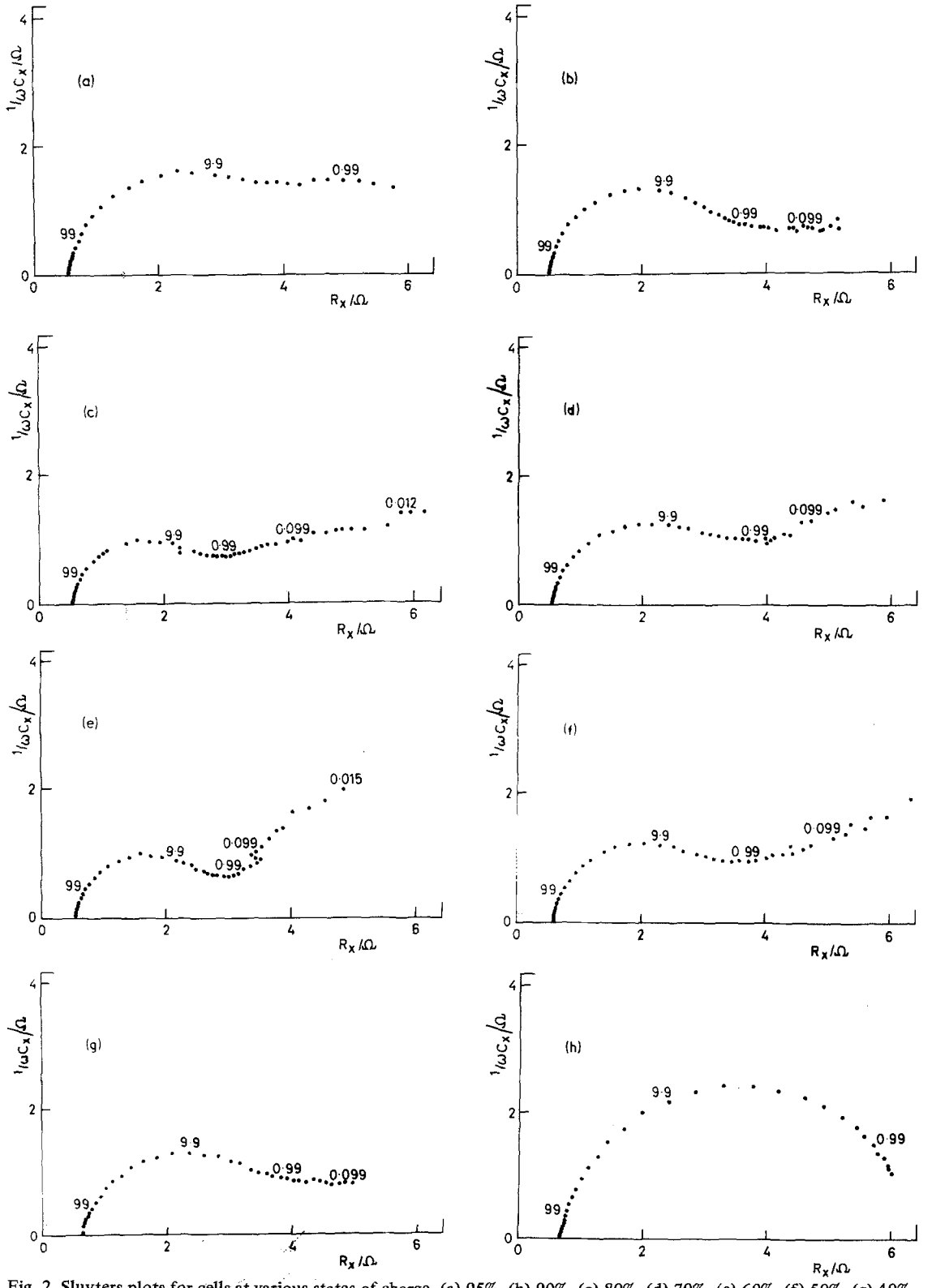

Fig. 2. Sluyters plots for cells at various states of charge. (a) 95%, (b) 90%, (c) 80%, (d) 70%, (e) 60%, (f) 50%, (g) 40%, (h) 30%. Numbers adjacent to points refer to frequency.

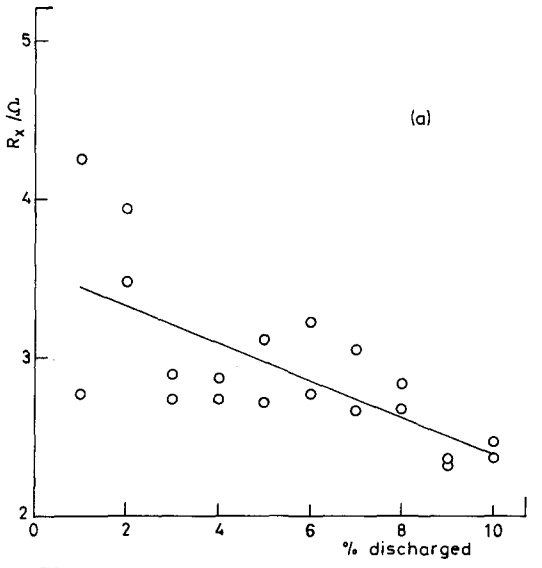
(a)
R_x /Ω
% discharged

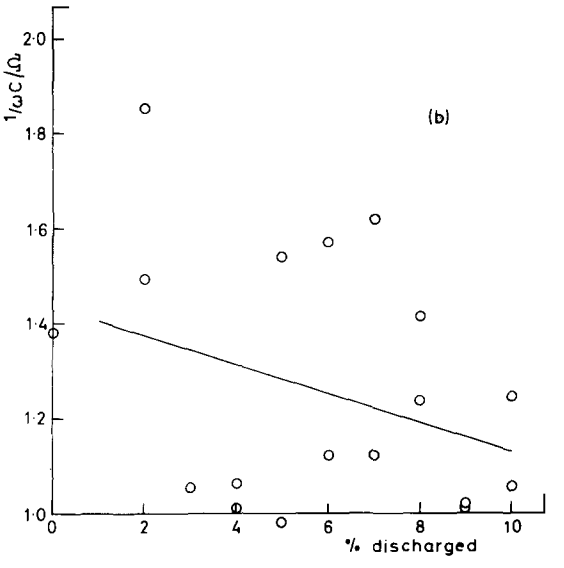
(b)
$1/\omega C$ /Ω
% discharged

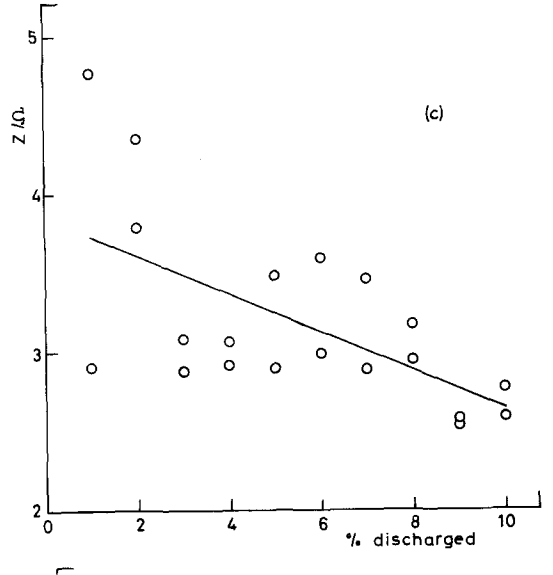
(c)
Z /Ω
% discharged

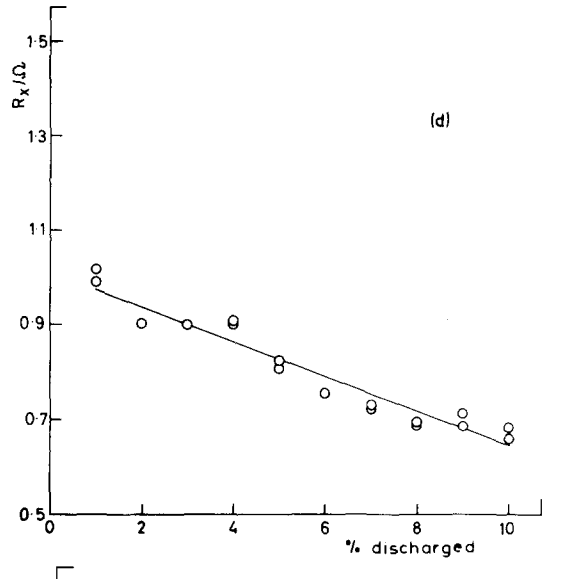
(d)
R_x /Ω
% discharged

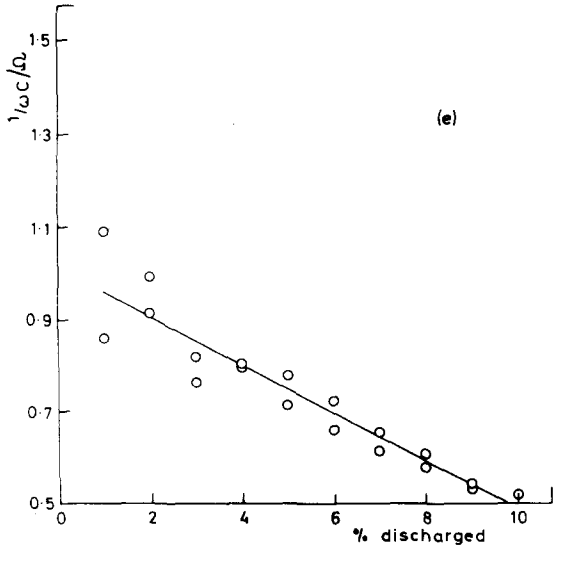
(e)
$1/\omega C$ /Ω
% discharged

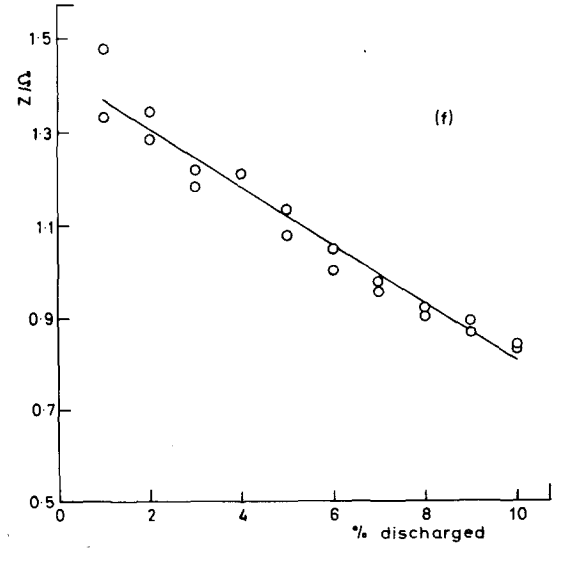
(f)
Z /Ω
% discharged

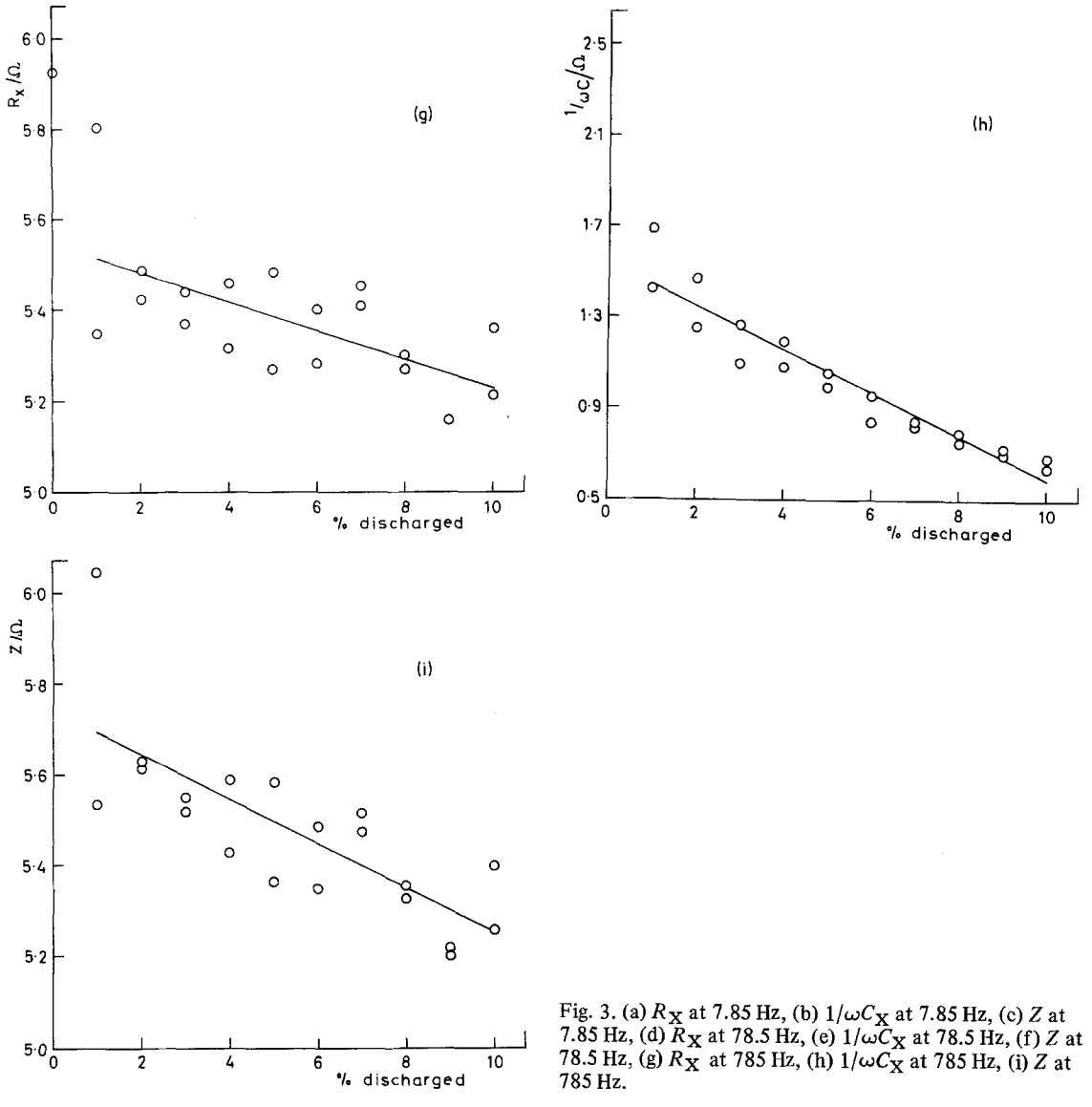

Fig. 3. (a) R_X at 7.85 Hz, (b) $1/\omega C_X$ at 7.85 Hz, (c) Z at 7.85 Hz, (d) R_X at 78.5 Hz, (e) $1/\omega C_X$ at 78.5 Hz, (f) Z at 78.5 Hz, (g) R_X at 785 Hz, (h) $1/\omega C_X$ at 785 Hz, (i) Z at 785 Hz.

high-frequency semicircle is characteristic of the charge-transfer reaction and connected with the exchange current for a well-defined planar electrode by

$$\theta = RT/ZFi_0$$

which we fully discussed in our earlier paper [2]. In this case the flattening of the semicircle is connected with the heterogeneity of the planar electrode and also with the porosity of the pitted electrode as we have discussed in [3].

The curves of Figs. 2a–h show how the impedance changes on discharging the cell. The form of the complex-plane plots is broadly the same throughout; however, the precise details of the shape alter as the cell is progressively drained. Although the diameter of the high-frequency semicircle does not change significantly over an extended charge range, there are some important changes which require comment.

The intercept on the resistance axis progressively increases throughout the discharge range. This is apparently connected with the development of high-conductivity products in the cell. The most likely site for this is the deposition of zinc oxide on the negative can electrode. This change is, however, small.

The low-frequency tail of the complex-plane

plot originally at 45° to the real axis for a fully-charged cell comes off at significantly lower angles as discharging continues but the behaviour does seem to approach a limit of approximately $\pi/8$ at around the 60% discharged level. This is confirmed visually by an examination of the surface of the zinc electrode at this point which was seen to be attacked at discrete points forming a pitted structure. Although these pits were not the circular pores of de Levie [6] they could well be the cause of the reduced slope of the low-frequency line.

The most important change in the impedance curves of Fig. 2 lies in the high-frequency semicircle and its degeneration into the straight line. This latter occurs at lower frequency as the discharging continues. The low-freqeuncy straight line joins the semicircle at points higher on the complex resistance plane as the extent of the discharge increases. The frequency range over which the semicircle extends moves to lower frequencies as discharging is carried out. We can interpret these changes as due to the reduction in the reaction rate due to change in reactant concentration. This thus gives rise to a decrease in frequency arising from the increase in θ. It is clear that there is no gross change in the electrochemical response with discharging, a conclusion which is confirmed by the relatively small change in open circuit voltage.

4. Development of the state-of-charge meter

The main region of interest in the present context extends from the fully charged Leclanché cell to a condition representing 10% discharged. Our results, Figs. 1 and 2, indicate that changes in the numerical value of the impedances are significant and should be capable of forming the basis of a satisfactory test device. It is clearly advantageous to identify the most useful parameter and conditions at which to carry out the test. Specifically the problem was to decide which of the impedance components (or the impedance itself), R or $1/\omega C$, provided the best assessment of state-of-charge and at what frequency. The criteria used were to search for that parameter which provided the most significant change with the least dispersion in the state-of-charge range 100–90%. The data retrieval capability of our frequency-response analyser was very high with the result that our experiments in the range had accumulated an enormous amount of information. The problem was tackled by filing all the available data in a computer and sorting for the most informative range by maximizing relative change with respect to per cent discharge at maximum correlation coefficient. Typical sorted outputs are shown in Figs. 3a–i which show the three quantities of interest over an extended frequency range 5 kHz down to 0.1 Hz. It is clear from these that the scatter of results about the mean curve is considerable and this scatter might vitiate any conclusions regarding the state of charge; consequently, the correlation coefficients of the parameter state-of-charge were plotted against the frequency. These are shown in Fig. 4, the curves displaying a maximum showing a strong correlation in a limited frequency region. The strongest correlation was found to exist in the resistance parameter at 31.2 Hz.

Fig. 5 shows the R parameter plotted against state-of-charge at 31.2 Hz together with the best straight line obtained using the method of least squares. We can see from this figure that the R factor changes by about 50% in the 100–90% region. This was considered to be an adequate change and formed the basis of our test. It was noteworthy that repeat cells gave exactly the same behaviour and this enabled us to proceed to the construction of the test set for state-of-charge assessment with considerable confidence.

The basic principles of operation of the test set may be explained with reference to the schematic diagram shown in Fig. 6. An oscillator generates a sinusoidally alternating voltage of fixed amplitude and a frequency of 31.2 Hz. The oscillator is connected via a switch to a current control and amplifier unit which feeds the battery under test, as shown. This unit delivers an output to an indicator which provides a digital or moving needle reading. A comparator operated by a ganged switch completes the arrangement. When the switch is connected to position 1, the indicator provides open-circuit voltage. When switched to position 2, the variable resistance R_R in the comparator is brought into play. R_R has values of resistance corresponding to those of the R parameter found from the computer study and its dial is calibrated in the associated values of percentage state-of-charge. R_R is adjusted until the indicator shows a minimum reading whereupon a

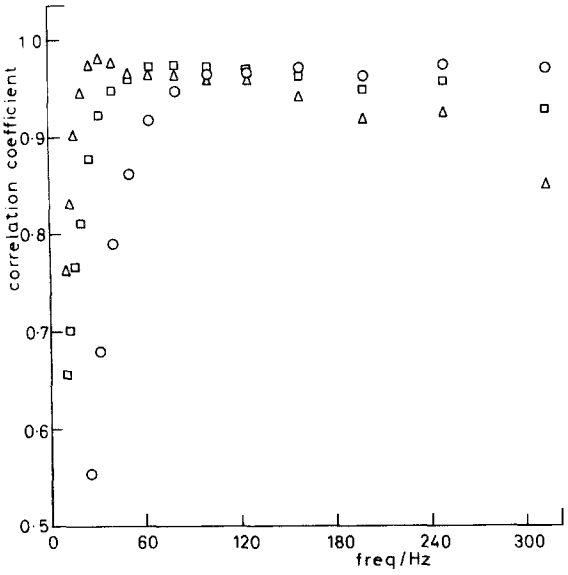

Fig. 4. Correlation coefficients of the parameters with state-of-charge plotted against frequency (0–10% discharged). △, R_X; ○, $1/\omega C$; □, Z.

pointer on R_R indicates the percentage state-of-charge on the dial. When switched to position 3, the values of the modulus of the impedance $|Z|$ found from the computer study are used to indicate percentage state-of-charge.

Although found to be the least reliable parameter, the capacitive reactance may be used as the reference parameter by switching to position 4 where the variable resistance R_X has ascribed to it the values of capacitive reactance corresponding to those found in the computer study and its dial is calibrated in percentage state-of-charge. The battery is fed with a suitably phase-advanced current and again R_X is adjusted until the indicator shows a minimum whereupon a pointer shows the percentage state-of-charge.

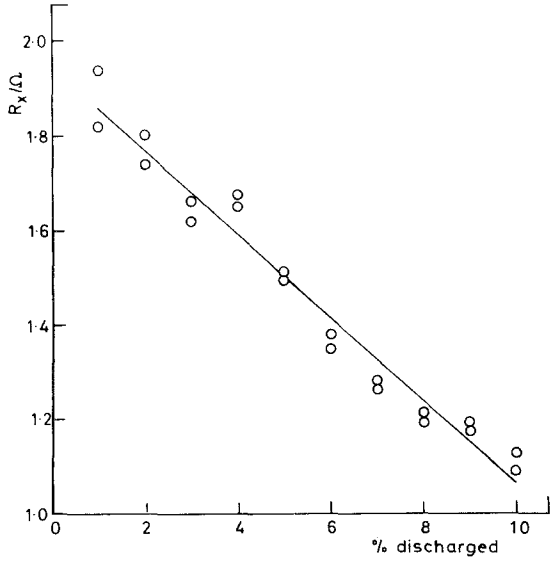

Fig. 5. R_X parameter against state-of-charge at 31.2 Hz.

In position 5 a variable resistance R_z has ascribed to it values corresponding to the modulus of the impedance '$|Z|$' found in the computer study and its dial is calibrated in percentage state-of-charge. The comparator feeds two independent currents into R_z. The vector sum of the two currents is kept constant but their ratio is made equal to the ratio of the mean-line values of resistance and reactance found in the computer study at each percentage state-of-charge marked on the dial of R_z. R_z is adjusted until the indicator shows a minimum, whereupon a pointer shows the state-of-charge.

In practice, the operation of the test set is simplified by ganging together the potentiometers on a single shaft with one pointer moving across a single dial calibrated in percentage state-of-charge which can be used for all switch positions. The prototype device has been constructed and shown to behave satisfactorily with test cells. Further development is being undertaken to perfect a device for convenient use (size, weight, robustness etc.) in the field; however, it is unlikely that the design shown in Fig. 6 will be modified significantly.

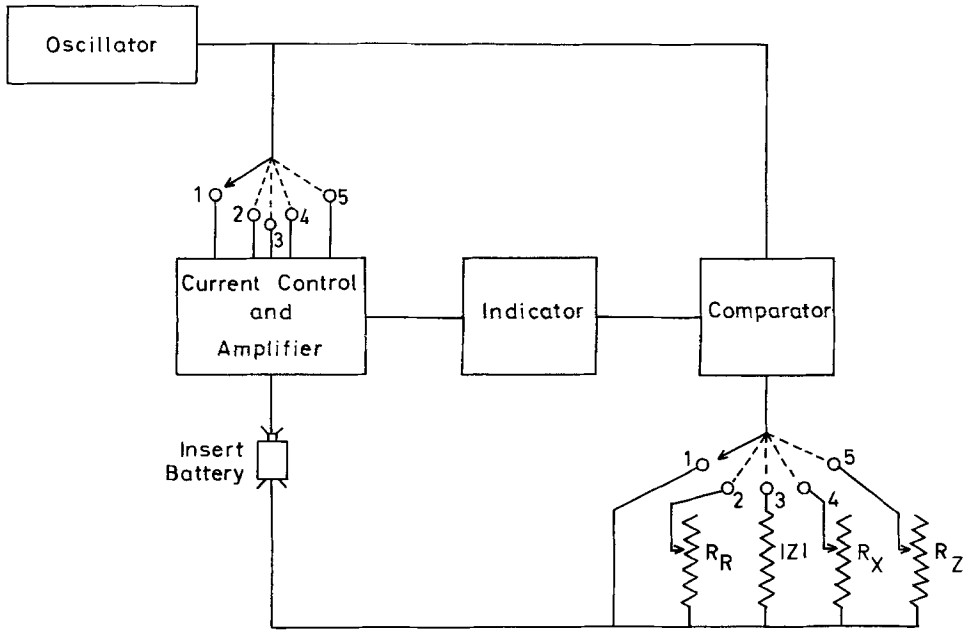

Fig. 6. The schematic diagram of a state-of-charge test set.

Acknowledgement

We thank the Procurement Executive of the Ministry of Defence for financial support to S. A. G. R. K.

References

[1] N. A. Hampson, S. A. G. R. Karunathilaka and R. Leek, *J. Appl. Electrochem.* **10** (1980) 3.

[2] S. A. G. R. Karunathilaka, N. A. Hampson, R. Leek and T. J. Sinclair, *ibid* **10** (1980) 357.

[3] *Idem, ibid* **10** (1980) 583.

[4] J. H. Sluyters, *Rev. Trav. Chim.* 79 (1960) 1092.

[5] J. E. B. Randles, *Disc. Faraday Soc.* 1 (1947) 11.

[6] R. de Levie, 'Advances in Electrochemistry and Electrochemical Engineering', Vol. 6 (edited by P. Delahay and C. W. Tobias) Interscience, New York (1967) p. 329.